Electronic Supplementary Information

Chlorocobaloxime Containing N-(4-pyridylmethyl)-1,8-naphthalamide Peripheral Ligands: Synthesis, Characterization and Enhanced Electrochemical Hydrogen Evolution in Alkaline Medium

Jitendra Kumar Yadav,[a] Baghendra Singh,[b] Sarvesh Kumar Pal,[a] Nanhai Singh,[a] Prem Lama,[c*] Arindam Indra[b*] and Kamlesh Kumar[a*]

[a]Department of Chemistry, Institute of Science, Banaras Hindu University, Varanasi 221005, India.

[b]Department of Chemistry, Indian Institute of Technology (BHU), Varanasi, UP-221005, India.

[c]CSIR Indian Institute of Petroleum, Tech Block, Mohkampur, Dehradun 248005, Uttarakhand, India.

*Corresponding authors:

E-mail: *kamlesh.kumar@bhu.ac.in (Kamlesh Kumar),*

Email: *prem.lama@iip.res.in (Prem Lama),*

Email: *arindam.chy@iitbhu.ac.in (Arindam Indra)*

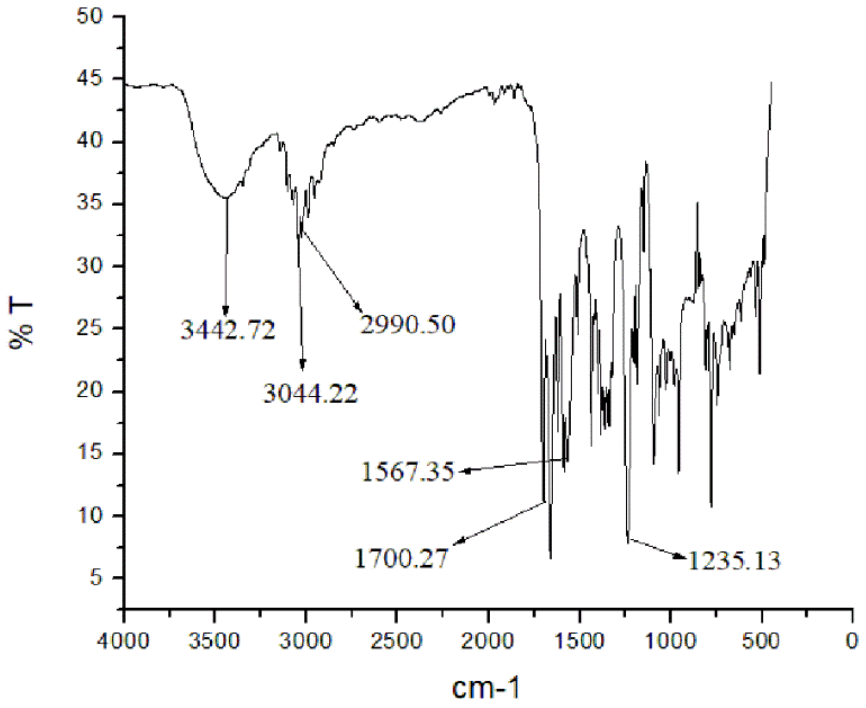

Figure S1: IR Spectrum of complex $[ClCo(dmgH)_2(L_1)]$ **(1)**

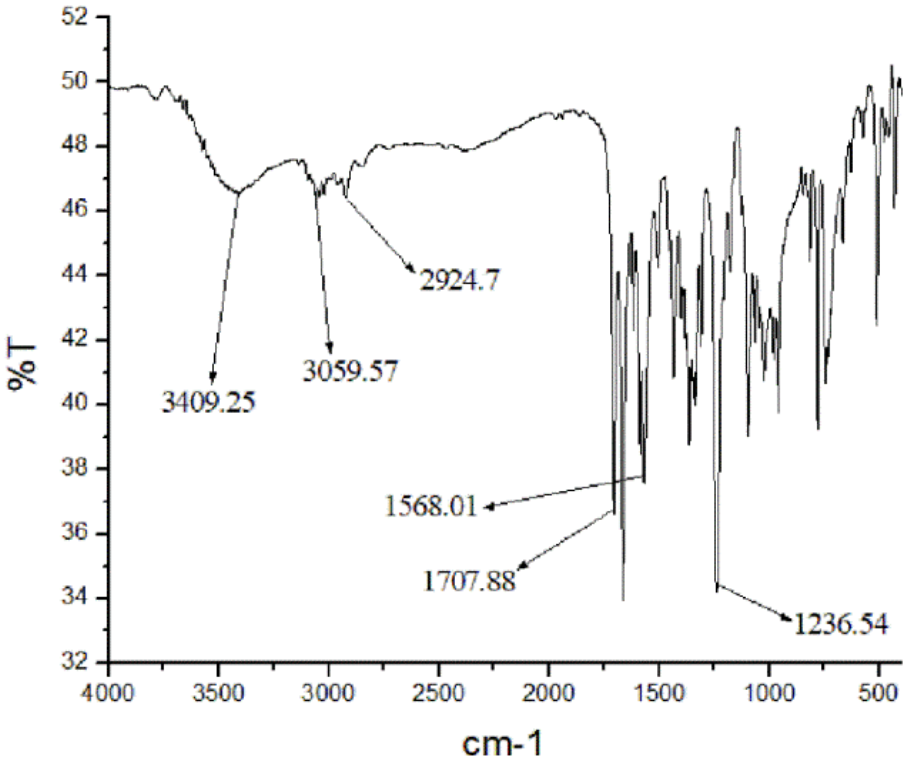

Figure S2: IR Spectrum of complex $[ClCo(dmgH)_2(L_2)]$ **(2)**

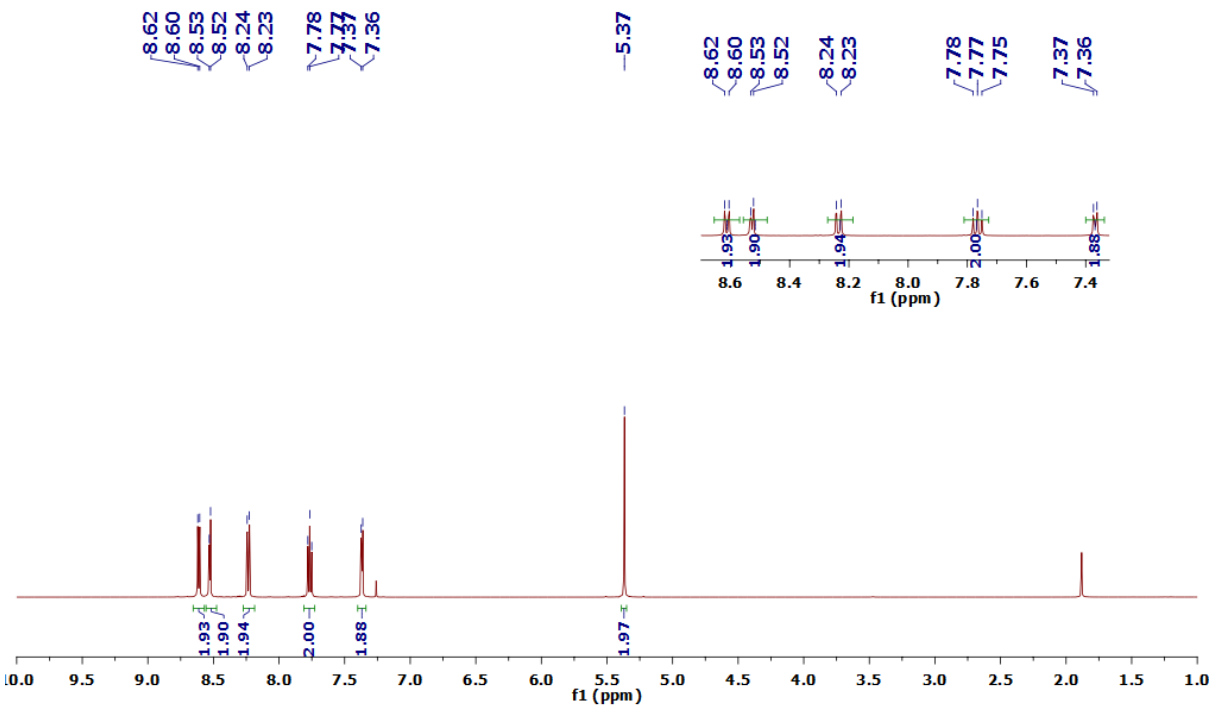

Figure S3: ^{1}H NMR spectrum (500 MHz, $CDCl_3$) of **L_1**

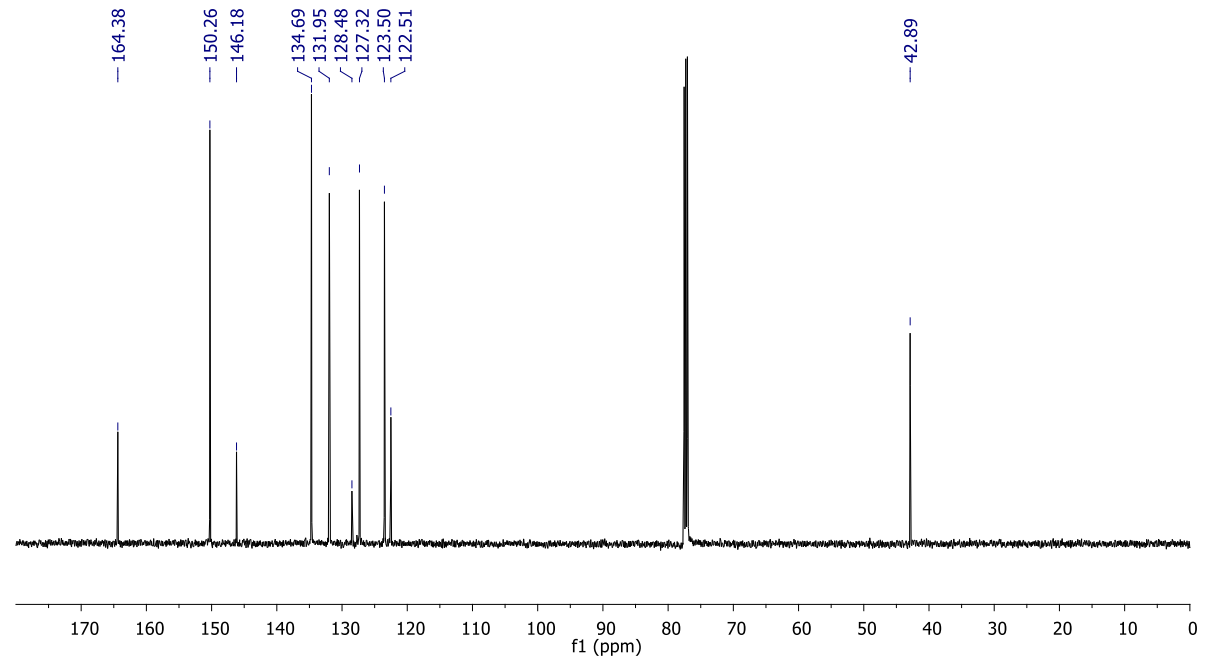

Figure S4: $^{13}C\{^{1}H\}$ NMR spectrum (125 MHz, $CDCl_3$) of **L_1**

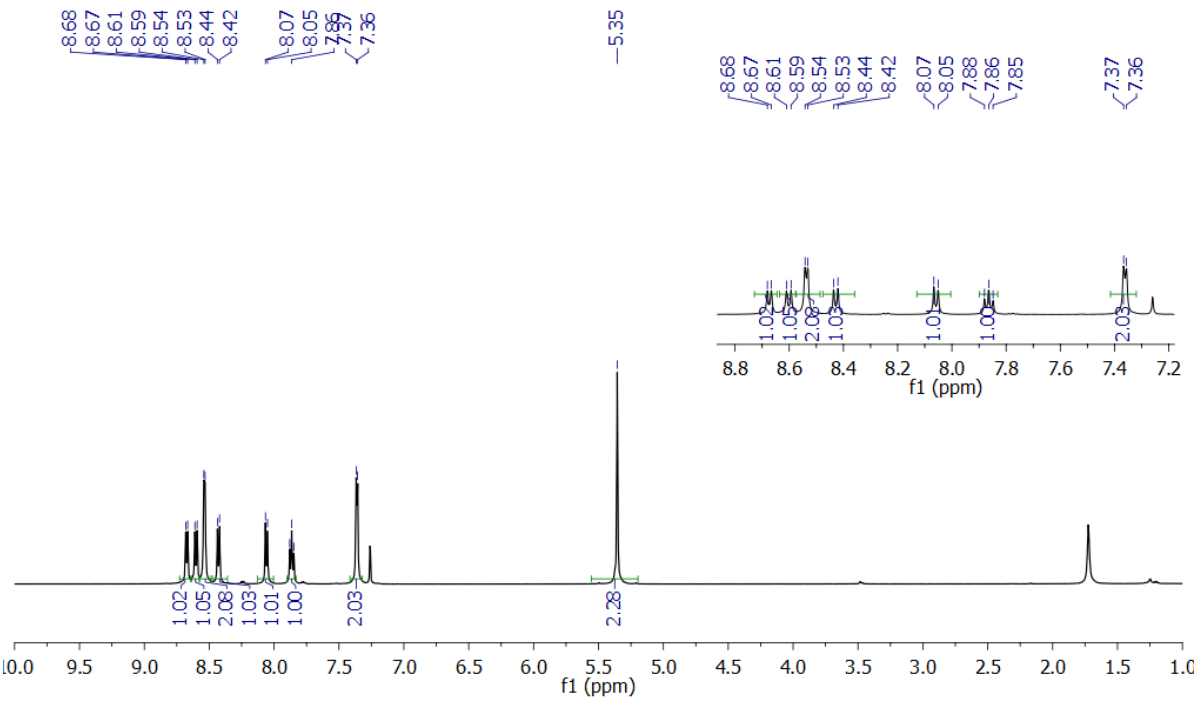

Figure S5: ^{1}H NMR spectrum (500 MHz, $CDCl_3$) of **L2**

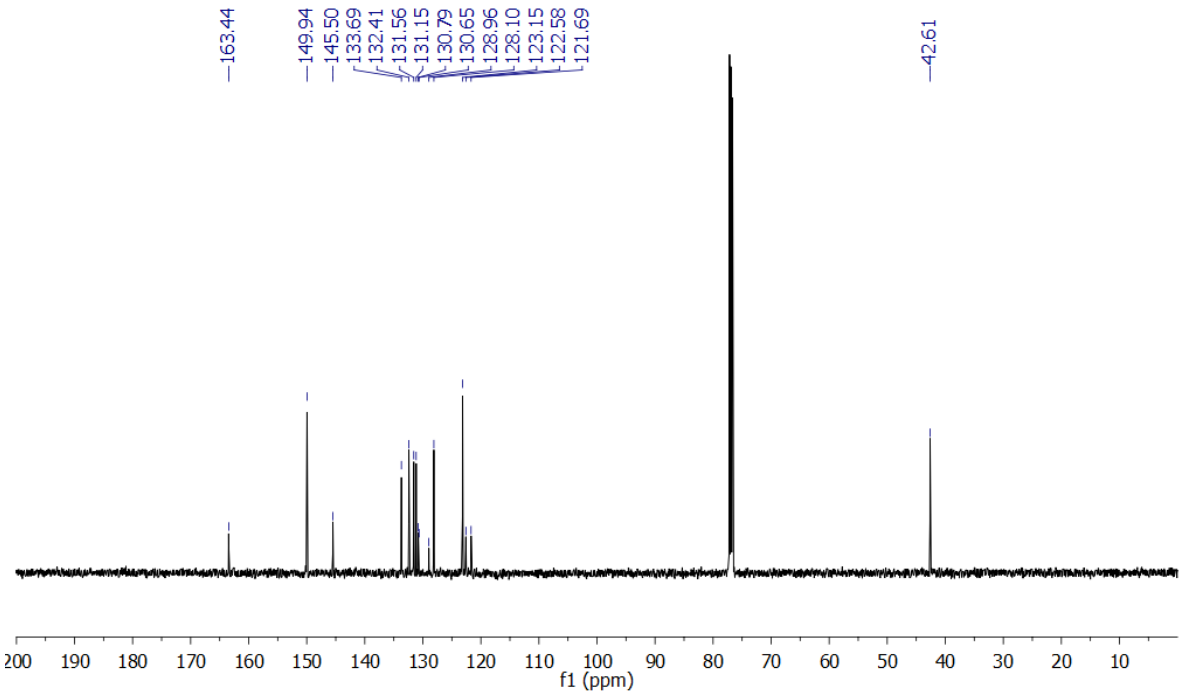

Figure S6: $^{13}C\{^{1}H\}$ NMR spectrum (125 MHz, $CDCl_3$) of **L2**

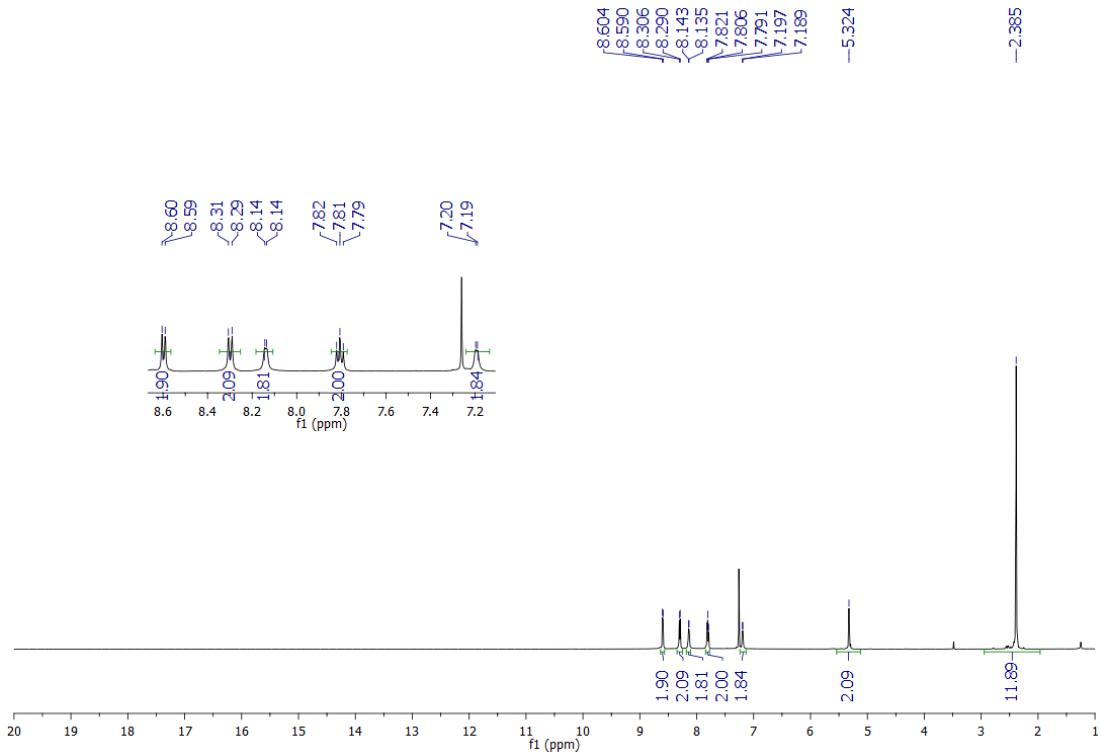

Figure S7: ^{1}H NMR spectrum (500 MHz, $CDCl_3$) of $[ClCo(dmgH)_2(L_1)]$ **(1)**

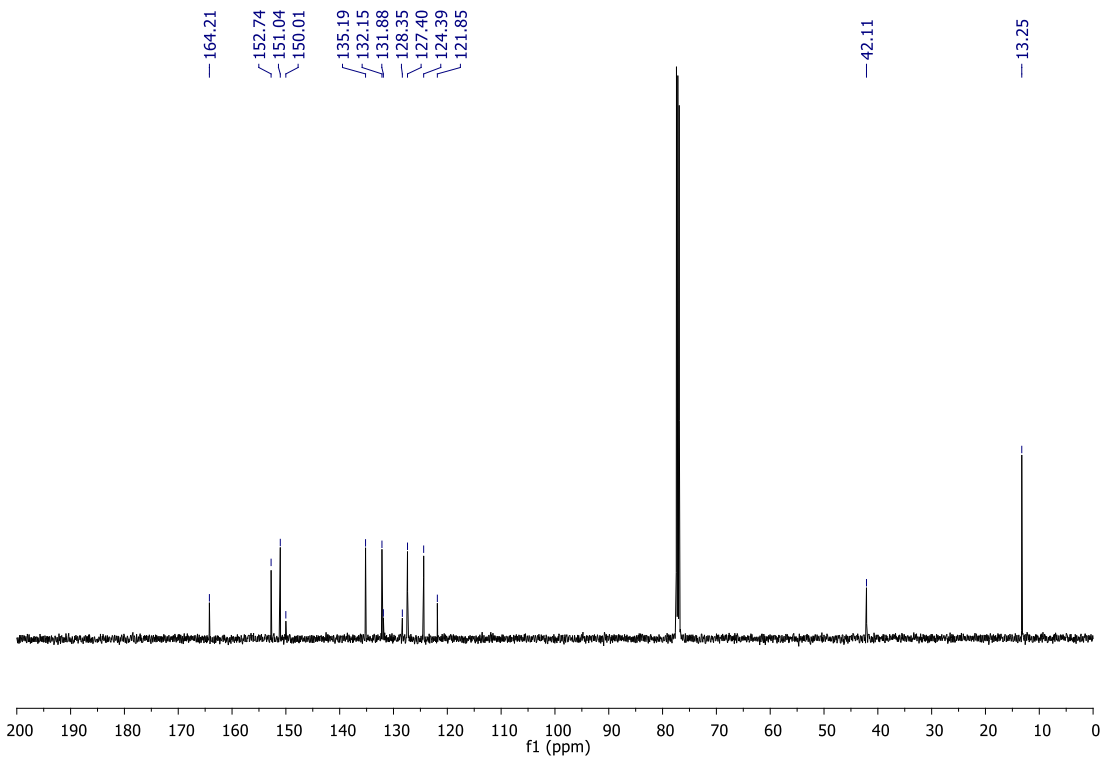

Figure S8: $^{13}C\{^{1}H\}$ NMR spectrum (125 MHz, CDCl3) of $[ClCo(dmgH)_2(L_1)]$ **(1)**

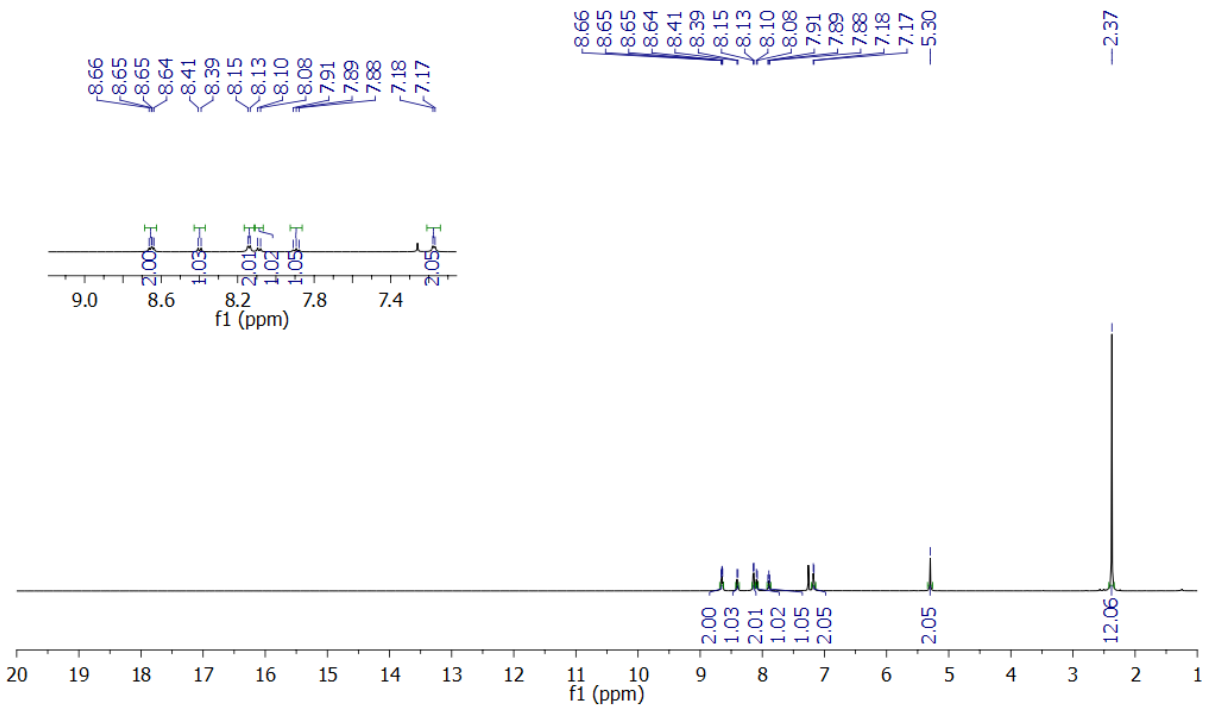

Figure S9: ^{1}H NMR spectrum (500 MHz, $CDCl_3$) of $[ClCo(dmgH)_2(L_2)]$ **(2)**

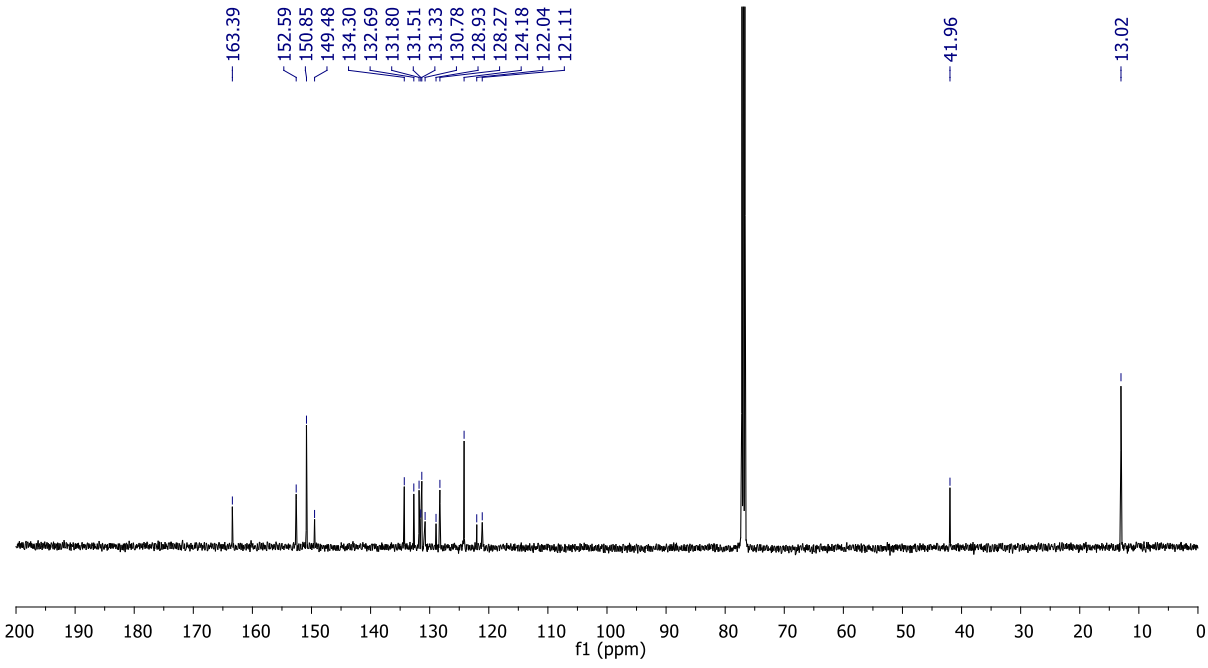

Figure S10: $^{13}C\{^{1}H\}$ NMR spectrum (125 MHz, $CDCl_3$) of $[ClCo(dmgH)_2(L_2)]$ **(2)**

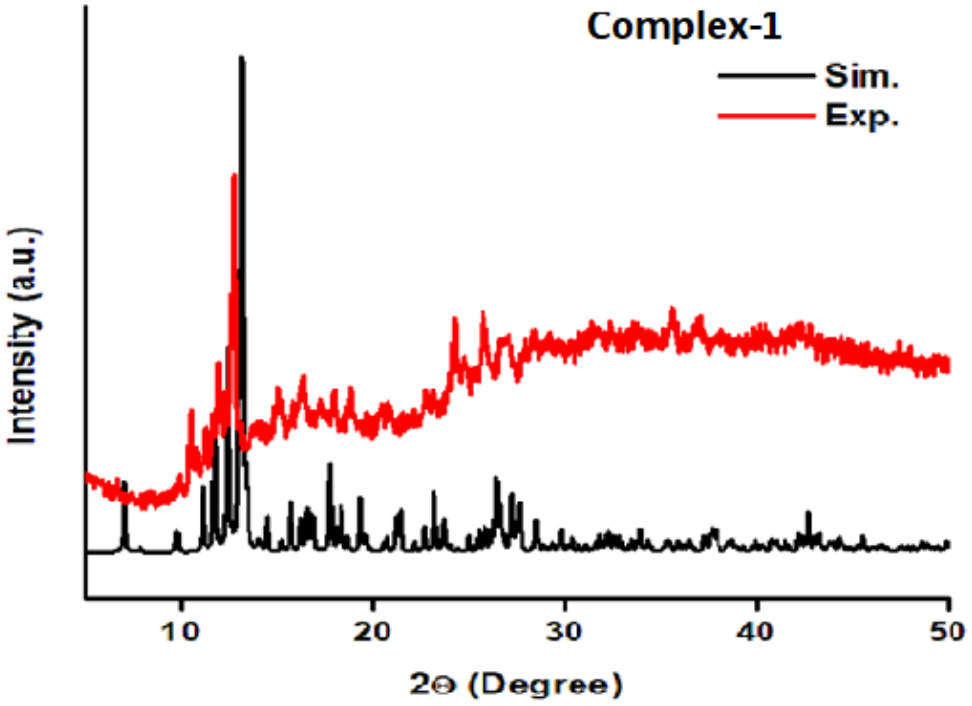

Figure S11: Simulated and experimental PXRD patterns of complex $[ClCo(dmgH)_2(L_1)]$ **(1)**

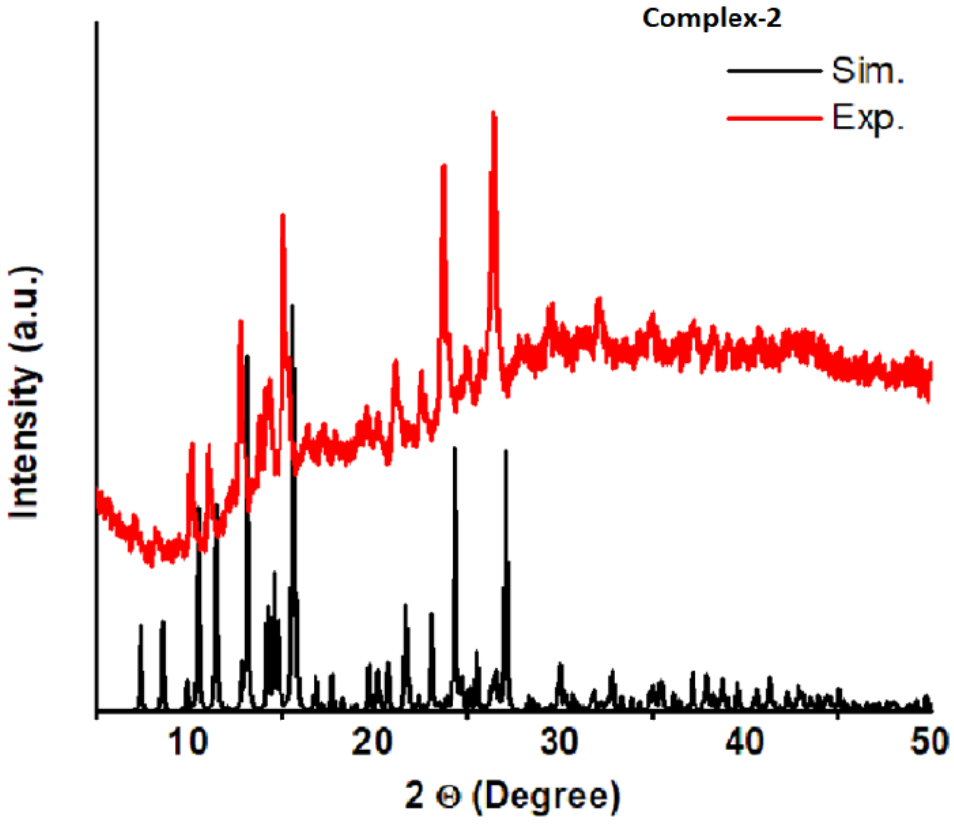

Figure S12: Simulated and experimental PXRD patterns of complex $[ClCo(dmgH)_2(L_2)]$ **(2)**

Table S1: Cobaloxime catalysed HER data. Overpotentials at a fixed current density (mA cm^{-2}) are reported in mV.

Sr. No.	Electrode	Cobaloxime Catalyst	Overpotential (mV)	Current density (mA cm^{-2})	Electrolyte	Ref
1	CNT	**Co-a**	590	-1	Acetate(pH 4.5)	*Nat. Chem.* **2013**, *5*, 48-53
2	CNT	**Co-b**	100	-2	Phosphate(pH 6.5)	*Angew. Chem., Int. Ed.* **2016**, *55*, 3952-3957
3	CNT	**Co-c**	100	-2	Phosphate (pH 6.5)	*Angew. Chem., Int. Ed.* **2016**, *55*, 3952-3957
4	Carbon cloth	**Co-d**	200	-4	acetate (pH 4.5)	*Chem. Commun*. **2015**, 51, 11508-11511
5	Carbon Cloth	**1**	435	-10	0.5 M H_2SO_4 (pH 0.13)	This work
6	Carbon Cloth	**1**	420	-1	Phosphate buffer (pH 6.61)	This work
7	Carbon Cloth	**1**	334	-10	1.0 M aqueous KOH solution (pH = 13.8)	This work
8	Carbon Cloth	**2**	409	-10	0.5 M H_2SO_4 (pH 0.13)	This work
9	Carbon Cloth	**2**	295	-1	Phosphate buffer (pH 6.61)	This work
10	Carbon Cloth	**2**	260	-10	1.0 M aqueous KOH solution (pH = 13.8)	This work

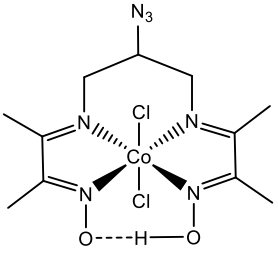

Co-a

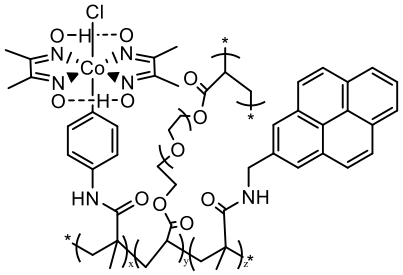

Co-c

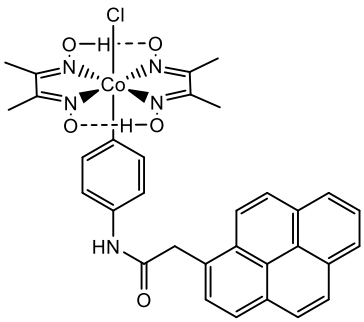

Co-b

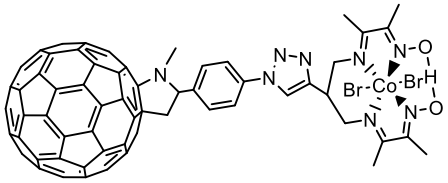

Co-d

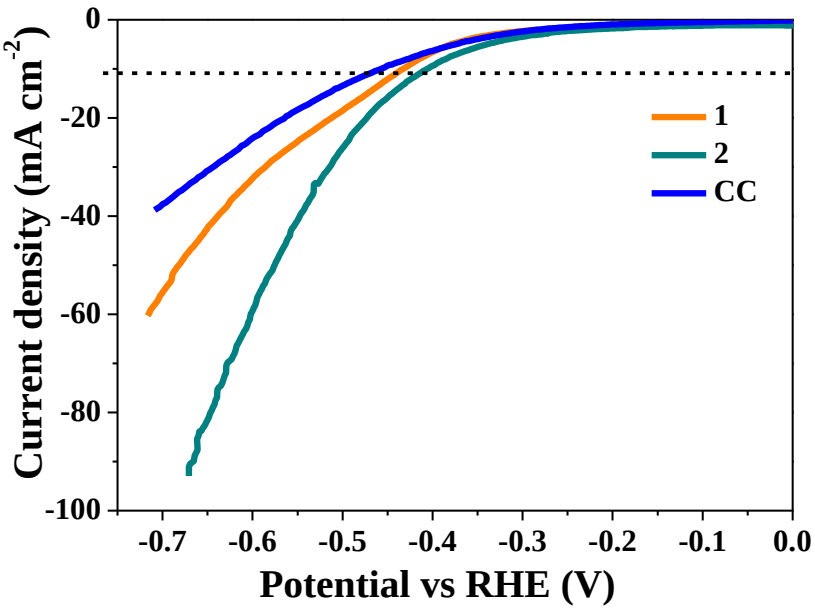

Figure S13. The linear sweep voltammetry (LSV) profile for the hydrogen evolution reaction (HER) of complex **1** and **2** compared with bare carbon cloth in 0.5 M H_2SO_4 (pH = 0.13, scan rate: 2 mV s^{-1}).

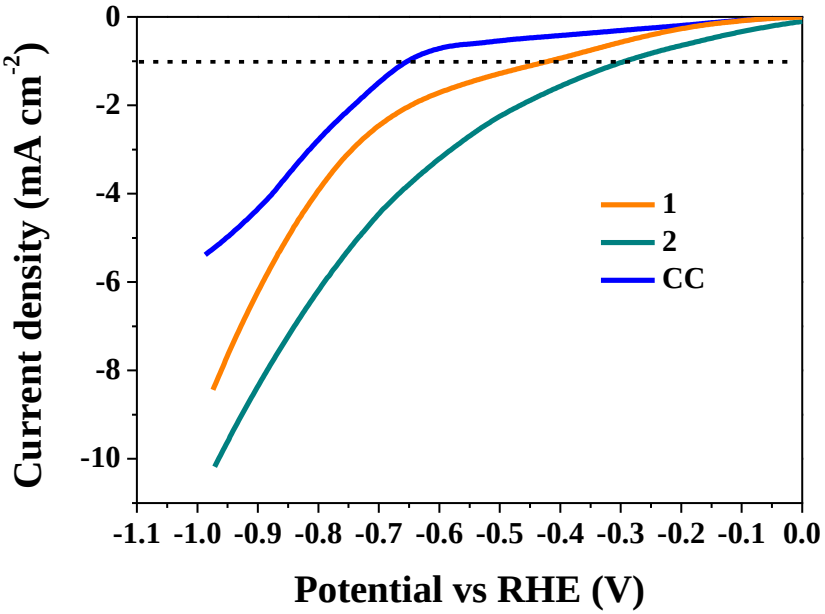

Figure S14. LSV profiles for the hydrogen evolution reaction of complex **1** and **2** compared with bare carbon cloth in phosphate buffer (pH = 6.61, scan rate: 2 mV s^{-1}).

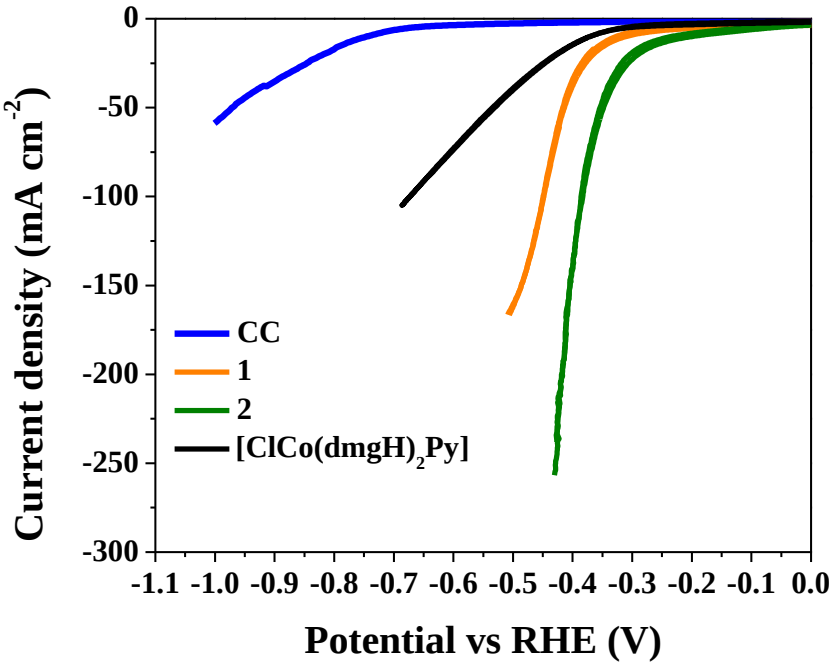

Figure S15. CV profile for the hydrogen evolution reaction of complexes **1** and **2** and [ClCo(dmgH)$_2$Py] compared with bare CC showing the enhanced HER activity for complex **1** and **2** as compared to [ClCo(dmgH)$_2$Py] in 1.0 M aqueous KOH solution (pH = 13.8, scan rate: 2 mV s^{-1}).

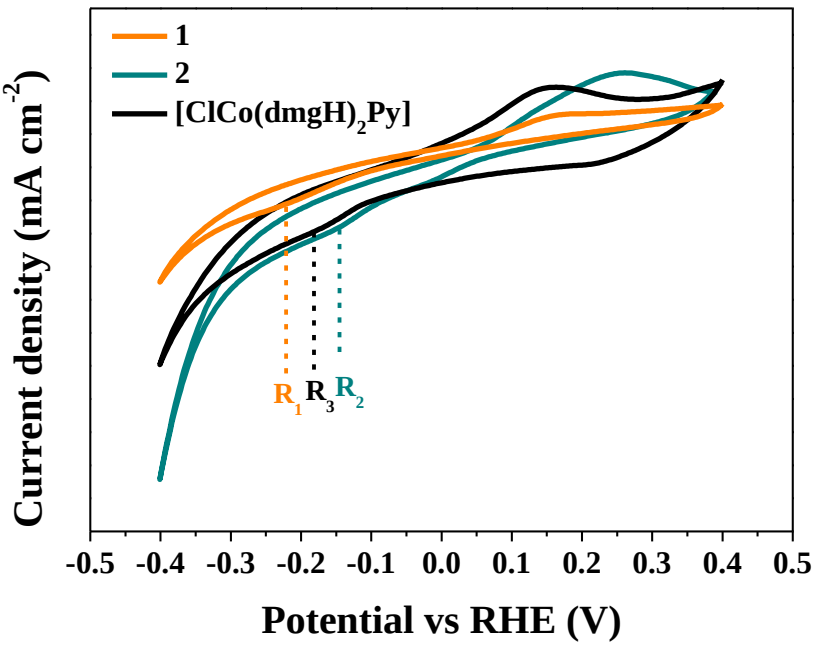

Figure S16. CV profiles of the complexes **1** and **2** and [ClCo(dmgH)$_2$Py] showing the redox peaks for the reduction of Co(II) to Co(I).electrolyte (pH = 13.8, scan rate: 2 mV s^{-1}).

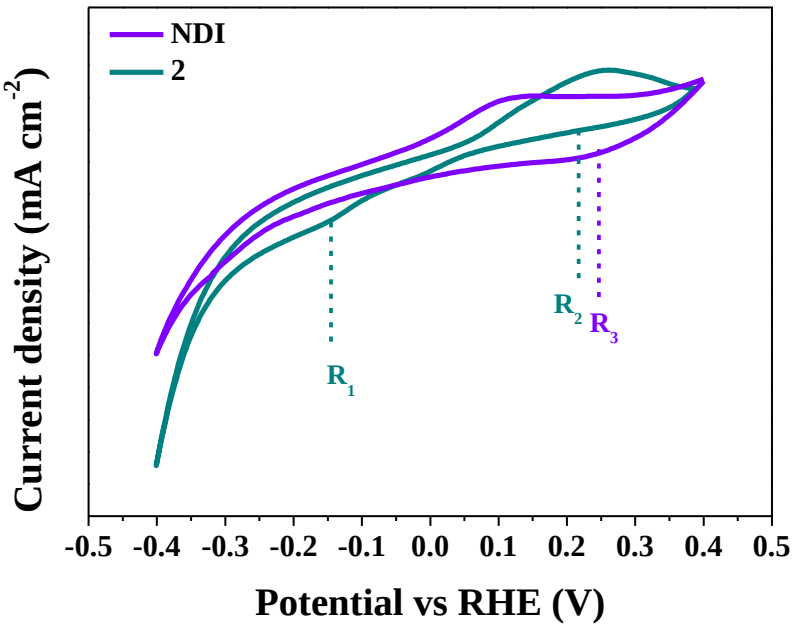

Figure S17. CV profiles of the complex **2** and ligand **NDI** (1.0 KOH, pH = 13.8, scan rate: 2 mV s^{-1}). The complex 2 showed the two reduction peaks for Co(II) to Co(I) (R_1) and NDI (R_2) while only one redox peak (R_3) was detected in **NDI**.

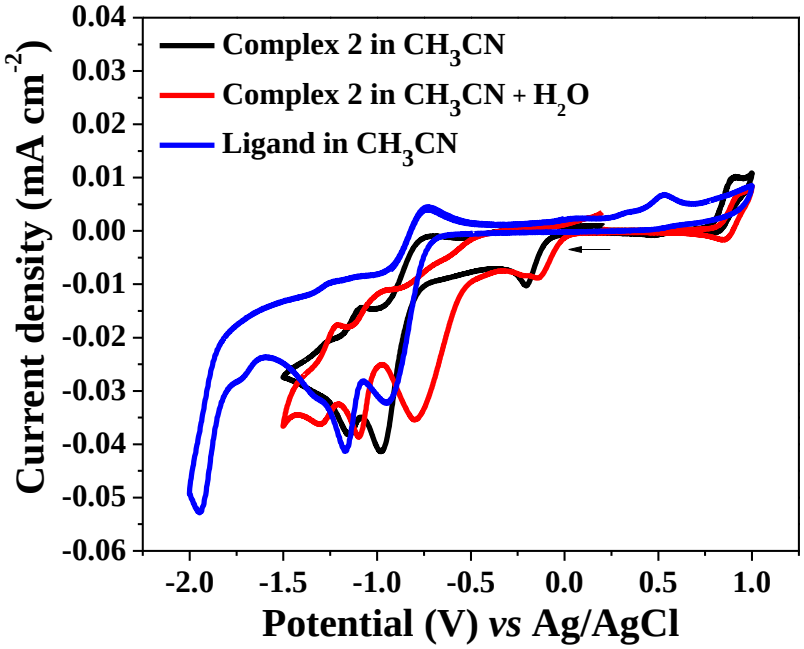

Figure S18. CV profiles of the complex **2** in acetonitrile and acetonitrile-water solution compared with CV of NDI ligand in acetonitrile (scan rate: 50 mV s^{-1} and supporting electrolyte is $[NBu_4][PF_6]$, glassy carbon working electrode).

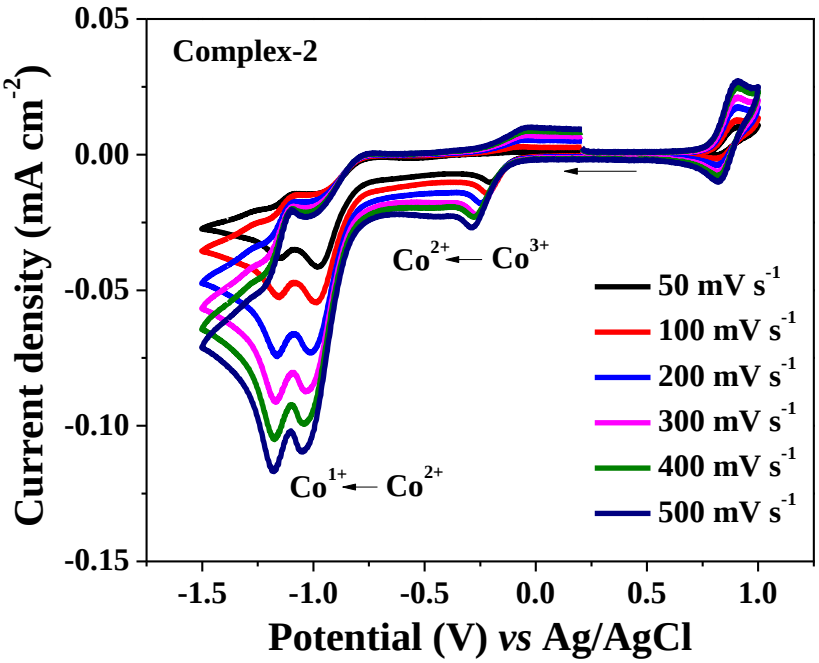

Figure S19. Scan rate dependent CV profiles of the complex **2** in acetonitrile solution. (Supporting electrolyte is $[NBu_4][PF_6]$, glassy carbon working electrode).

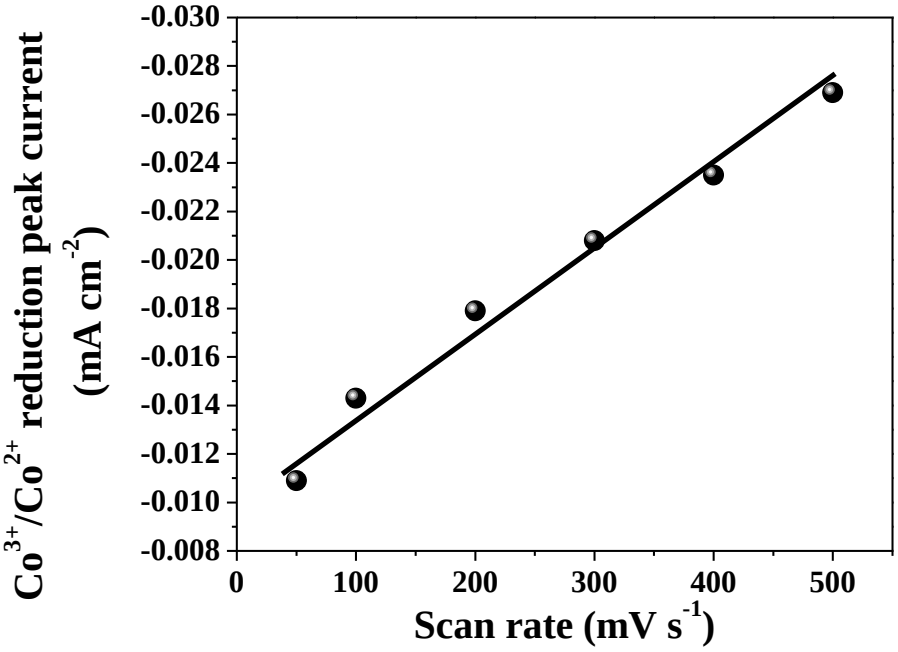

Figure S20. Co^{3+}/Co^{2+} reduction peak current of complex **2** plotted against varying scan rates.

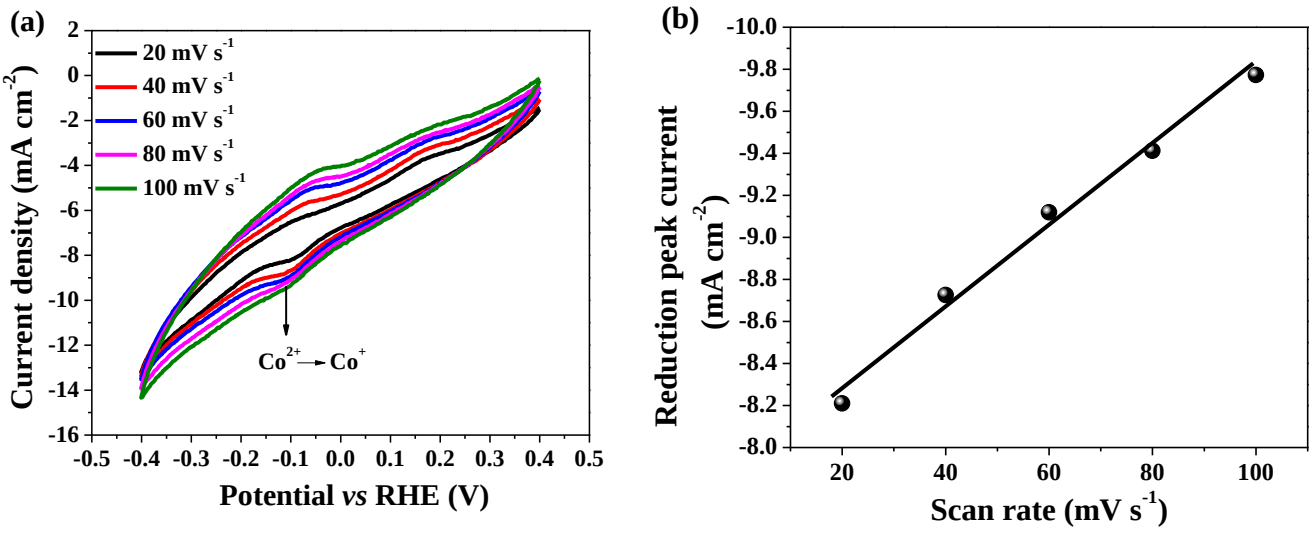

Figure S21. (a) Scan rate dependent CV profiles of complex **2** immobilized on carbon cloth in 1.0 M KOH solution and (b) plot of the reduction peak current density with varying scan rates.

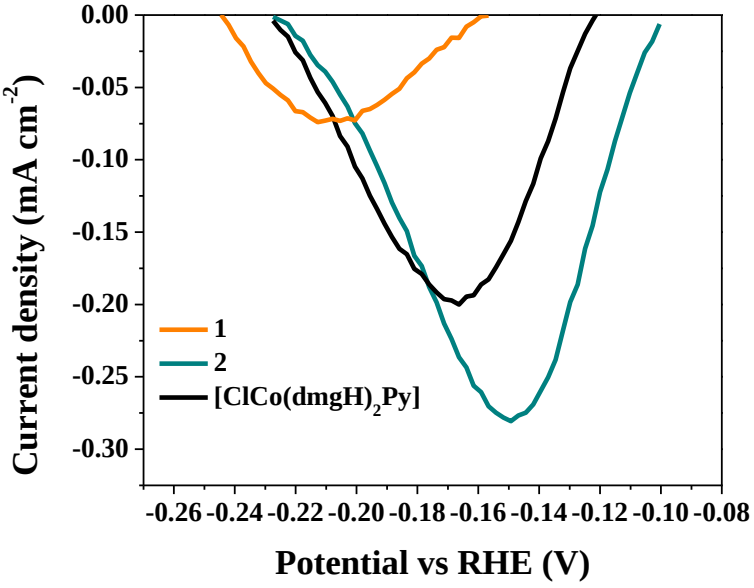

Figure S22. Reduction peak area (R_1, R_2, R_3) of the complexes **1** and **2** and [ClCo(dmgH)$_2$Py], respectively utilized for the calculation of electroactive species by the integration of reduction peak.

Equation S2. Determination of surface concentration of electroactive species

We have determined the surface concentration of the electroactive species in mol/cm^2 using the Sharp equation.[1-2] The peak current under CV is related to the surface concentration of electroactive species (Γ) by the following equation:[1-2]

$$I_p = n^2F^2A\Gamma v / 4RT$$

$$\Gamma = I_p 4RT / n^2F^2A\Gamma v$$

where n represents the number of electrons involved in the reaction, A is the geometric surface area of the electrode, Γ is the surface concentration of the electroactive species (mol cm^{-2}), v is the scan rate (V s^{-1}), R denote the gas constant (8.314 J mol^{-1} K^{-1}), F represents the Faraday constant (96 485 C mol^{-1}) and T express the temperature (298 K).[1-2]

For complex **2**

$$\Gamma = 0.279 \text{ x } 4 \text{ x } 8.314 \text{ x } 298 / 2^2 \text{ x } 96485 \text{ x } 1 \text{ x } 0.005$$

$$\mathbf{\Gamma = 1.48 \text{ x } 10^{-5} \text{ mol cm}^{-2}}$$

For complex **1**

$$\Gamma = 0.199 \text{ x } 4 \text{ x } 8.314 \text{ x } 298 / 2^2 \text{ x } 964852 \text{ x } 1 \text{ x } 0.005$$

$$\mathbf{\Gamma = 1.05 \text{ x } 10^{-5} \text{ mol cm}^{-2}}$$

For complex [ClCo(dmgH)$_2$Py]

$$\Gamma = 0.072 \text{ x } 4 \text{ x } 8.314 \text{ x } 298 / 2^2 \text{ x } 964852 \text{ x } 1 \text{ x } 0.005$$

$$\mathbf{\Gamma = 0.38 \text{ x } 10^{-5} \text{ mol cm}^{-2}}$$

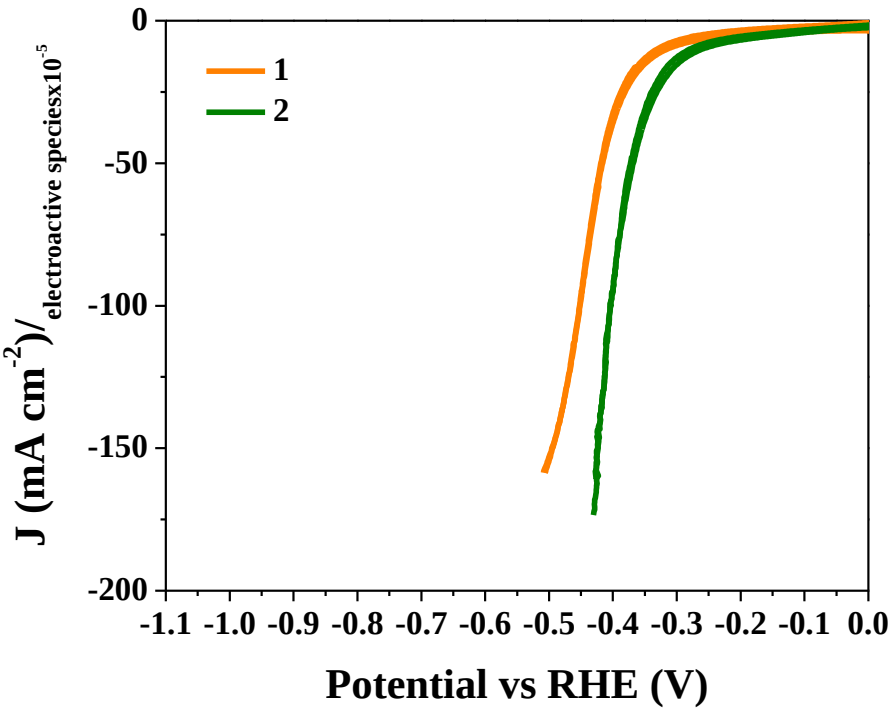

Figure S23. The HER activity of the complexes **1** and **2** normalized with the surface concentration of electroactive sites.

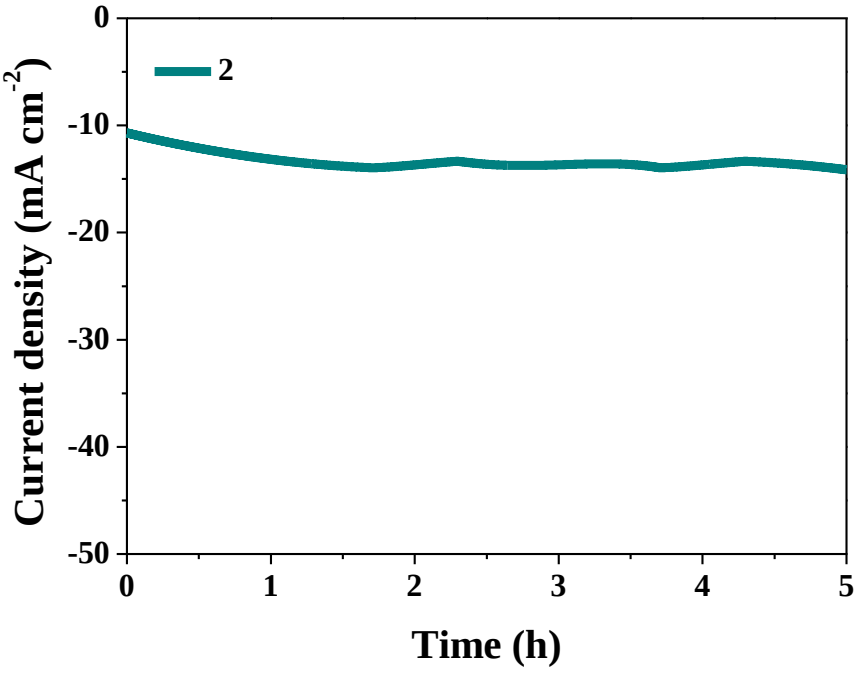

Figure S24. Chronoamperometric measurement for the hydrogen evolution reaction of complex **2** at 280 mV overpotential showing the stability of complex **2** for 5 h.

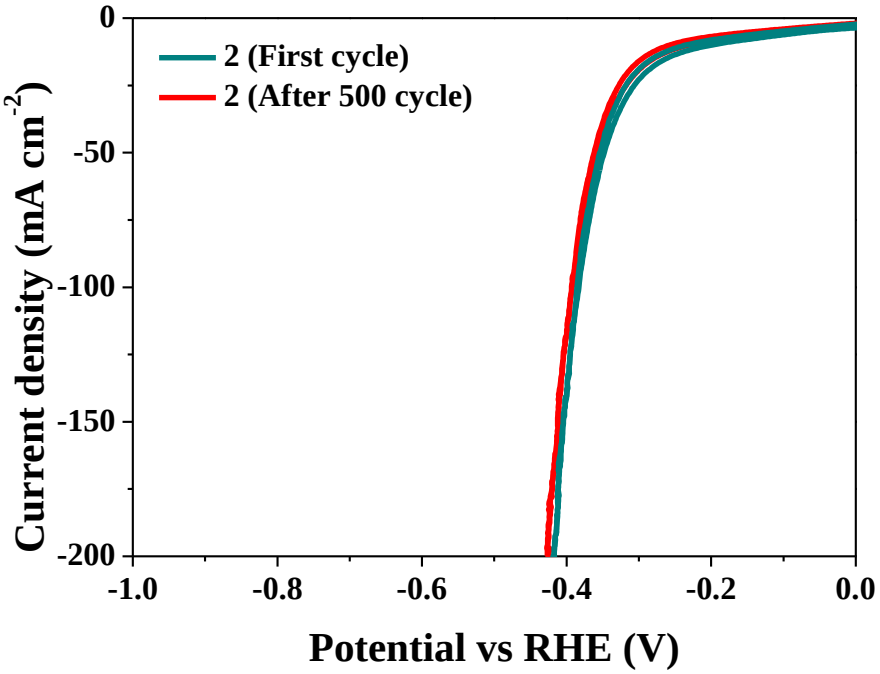

Figure S25: CV profile for the hydrogen evolution reaction of complex **2** for first cycle and after 500 CV cycles showing no change in the overpotential as well as in current density after 500 CV cycles.

Determination of the faradaic efficiency of complex 2

The water displacement method has been utilized to determine the amount of hydrogen produced during the hydrogen evolution reaction. The amount of H_2 was detected during the chronoamperometric measurement for 3600 s at 10 mA cm^{-2} current density.[3-5] Firstly, the theoretical calculated amount of hydrogen was calculated using the following equation from Faraday's law.[3-5]

$$nH_2\,(\text{theoretical}) = \frac{Q}{n \times F} = \frac{I \times t}{n \times F} = \frac{0.02\ A \times 3600\ s}{2 \times 96485.3\ s\ A\ mol^{-1}} = 0.00037\ mmol$$

Where nH_2 represents the theoretically calculated amount of H_2, Q denotes amount of applied charge, *n* shows the number of electrons transferred in HER (2 electrons), *F* denotes the Faraday constant (96485.3 s A mol^{-1}), *I* represents the applied current (0.01 A), and *t* is the reaction time (3600 s).[3-5]

At the time of chronoamperometric measurements, the amount of hydrogen generated during the experiment was measured and the theoretically calculated amount was compared with the actually generated amount of H_2. Further, the faradaic efficiency was calculated using the following equation: [3-5]

$$\text{Faradaic efficiency}\,(\%) = \frac{nH_2\,(\text{experimental})}{nH_2\,(\text{Theoretical})} \times 100 = \frac{0.000365\ mmol}{0.00037\ mmol} \times 100 = 98.6\%$$

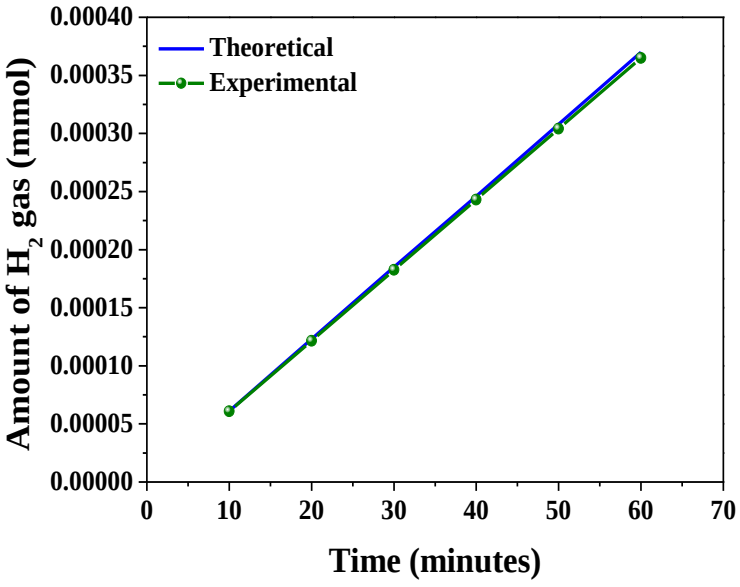

Figure S26. Plot for the amount of theoretically calculated hydrogen (blue line) and experimentally measured hydrogen (green line) versus time for complex **2**.

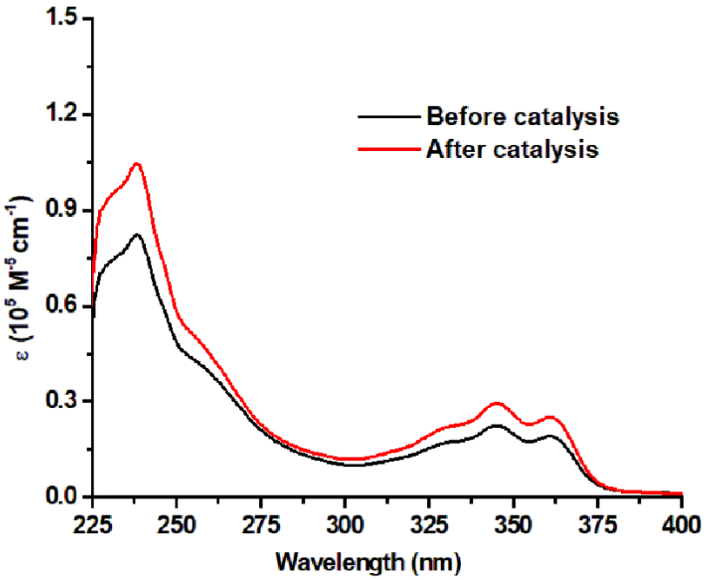

Figure S27. UV-Vis spectra of complex **2 (**After and before the catalysis) in CH_2Cl_2 solution at 10^{-5} molar concentration.

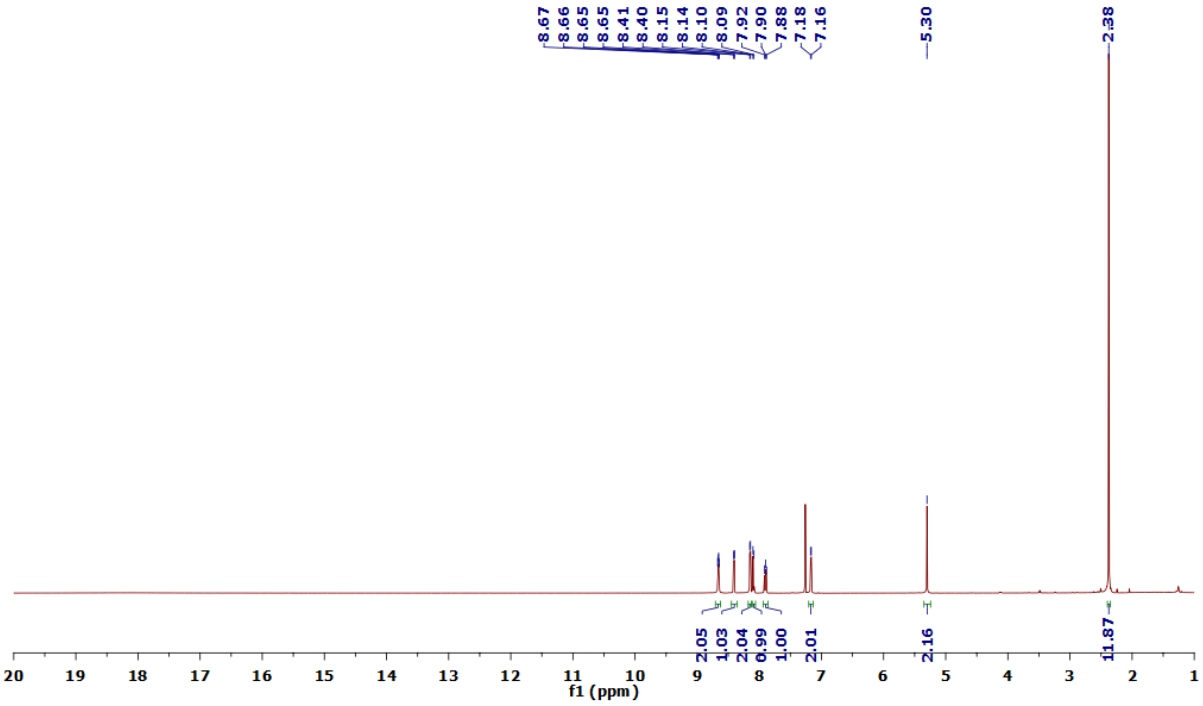

Figure S28: ^{1}H NMR spectrum (500 MHz, $CDCl_3$) of complex **2** after electrochemical hydrogen evolution in 1.0 M aqueous KOH solution.

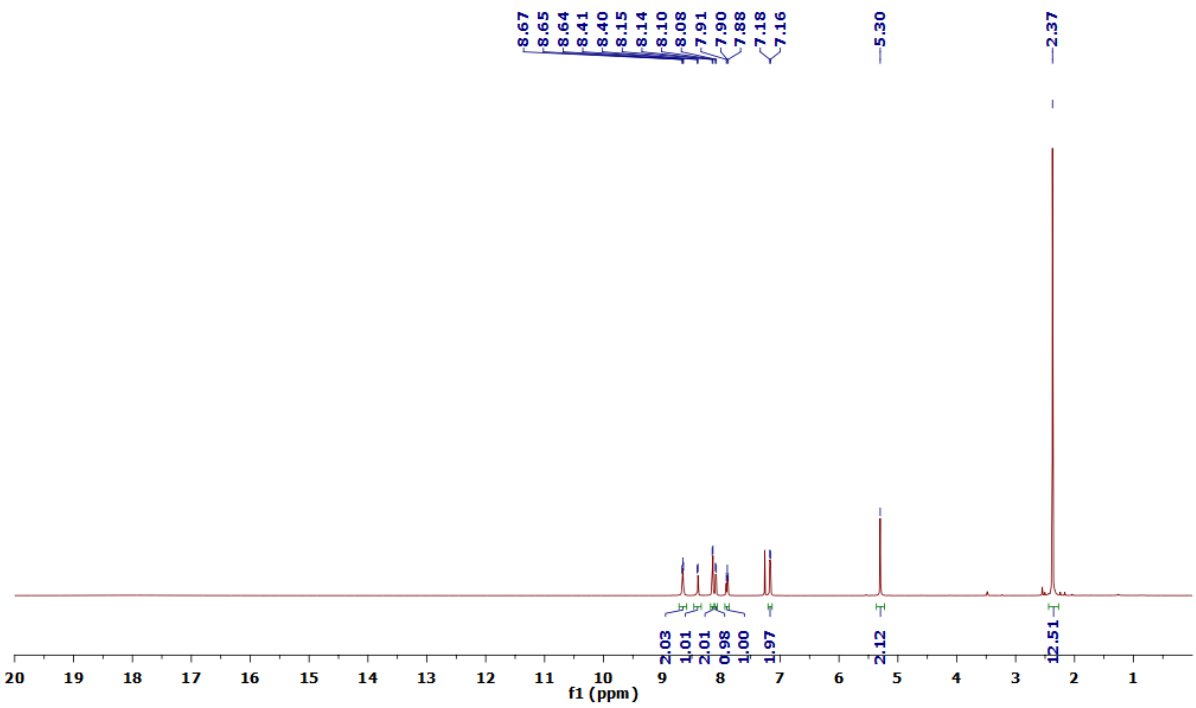

Figure S29: ^{1}H NMR spectrum (500 MHz, $CDCl_3$) of complex **2** after dipping in 1.0 M aqueous KOH solution for 2 h.

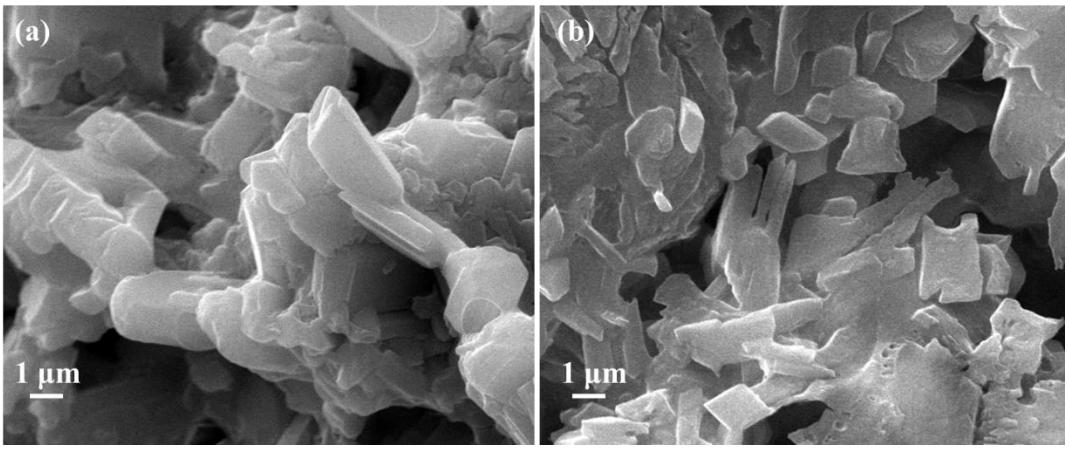

Figure S30: (a) SEM image of complex **2** before HER catalysis (fresh) and (b) SEM image of complex **2** after 5 h chronoamperometric HER showing no change in the morphology after catalysis.

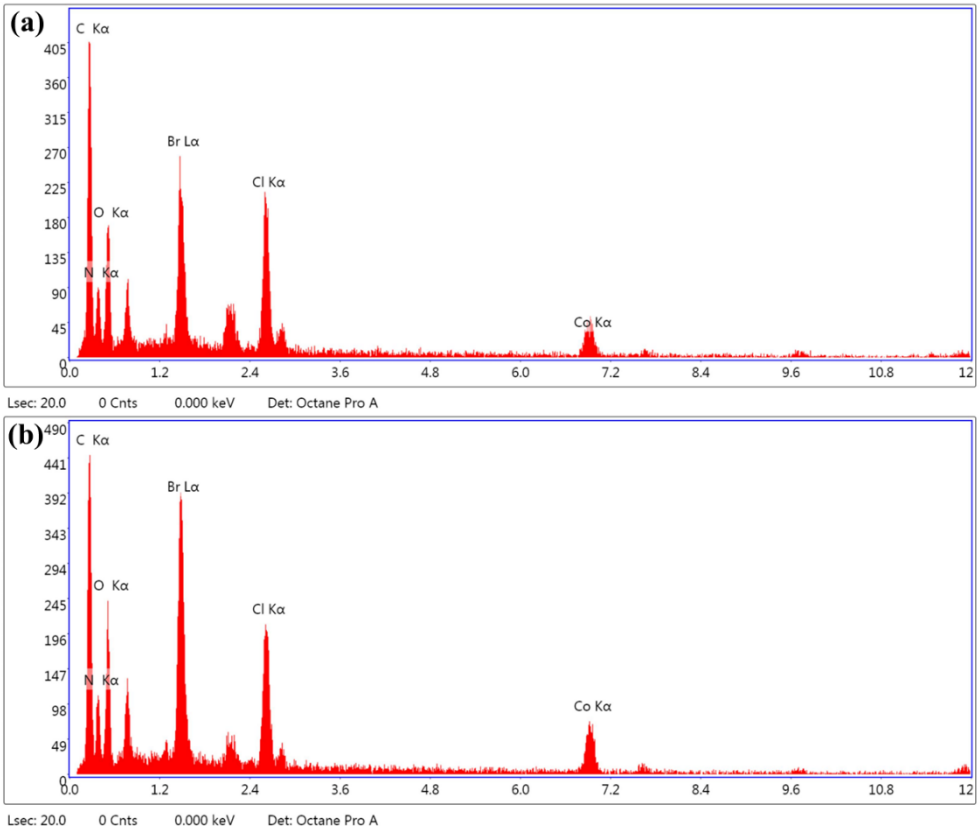

Figure S31: (a) EDX spectra of complex **2** before HER catalysis (fresh) and (b) EDX spectra of complex **2** after 5 h chronoamperometric HER.

References

1. M. Tohidinia, A. Biabangarda and M. Noroozifar, *RSV Adv*., 2020, **10**, 2944–2951.
2. A. L. Eckermann, D. J. Feld, J. A. Shaw and T. J. Meade, *Coord. Chem. Rev*., 2010, **254**, 1769–1802
3. J. Jia, L. C. Seitz, J. D. Benck, Y. Huo, Y. Chen, J. W. D. Ng, T. Bilir, J. S. Harris and T. F. Jaramillo, *Nat. Commun*., 2016, **7**, 13237.
4. A. Paracchino, V. Laporte, K. Sivula, M. Grätzel and E. Thimsen, *Nat. Mater*., 2011, **10**, 456-461.
5. I. M. Mosa, S. Biswas, A. M. El-Sawy, V. Botu, C. Guild, W. Song, R. Ramprasad, J. F. Ruslingace and S. L. Suib, *J. Mater. Chem. A*, 2016, **4**, 620-631.